Juvenile salmon acoustic monitoring in the Discovery Islands, British Columbia

S. Rousseau, S. Gauthier, S. Johnson
C. Neville and M. Trudel

Fisheries and Oceans Canada
Science Branch, Pacific Region
9860 West Saanich Road
Sidney, BC, Canada
V8L 4B2

2018

Canadian Technical Report of Fisheries and Aquatic Sciences 3277

Fisheries and Oceans Canada | Pêches et Océans Canada

Canada

Canadian Technical Report of Fisheries and Aquatic Sciences

Technical reports contain scientific and technical information that contributes to existing knowledge but which is not normally appropriate for primary literature. Technical reports are directed primarily toward a worldwide audience and have an international distribution. No restriction is placed on subject matter and the series reflects the broad interests and policies of Fisheries and Oceans Canada, namely, fisheries and aquatic sciences.

Technical reports may be cited as full publications. The correct citation appears above the abstract of each report. Each report is abstracted in the data base Aquatic Sciences and Fisheries Abstracts.

Technical reports are produced regionally but are numbered nationally. Requests for individual reports will be filled by the issuing establishment listed on the front cover and title page.

Numbers 1-456 in this series were issued as Technical Reports of the Fisheries Research Board of Canada. Numbers 457-714 were issued as Department of the Environment, Fisheries and Marine Service, Research and Development Directorate Technical Reports. Numbers 715-924 were issued as Department of Fisheries and Environment, Fisheries and Marine Service Technical Reports. The current series name was changed with report number 925.

Rapport technique canadien des sciences halieutiques et aquatiques

Les rapports techniques contiennent des renseignements scientifiques et techniques qui constituent une contribution aux connaissances actuelles, mais qui ne sont pas normalement appropriés pour la publication dans un journal scientifique. Les rapports techniques sont destinés essentiellement à un public international et ils sont distribués à cet échelon. II n'y a aucune restriction quant au sujet; de fait, la série reflète la vaste gamme des intérêts et des politiques de Pêches et Océans Canada, c'est-à-dire les sciences halieutiques et aquatiques.

Les rapports techniques peuvent être cités comme des publications à part entière. Le titre exact figure au-dessus du résumé de chaque rapport. Les rapports techniques sont résumés dans la base de données Résumés des sciences aquatiques et halieutiques.

Les rapports techniques sont produits à l'échelon régional, mais numérotés à l'échelon national. Les demandes de rapports seront satisfaites par l'établissement auteur dont le nom figure sur la couverture et la page du titre.

Les numéros 1 à 456 de cette série ont été publiés à titre de Rapports techniques de l'Office des recherches sur les pêcheries du Canada. Les numéros 457 à 714 sont parus à titre de Rapports techniques de la Direction générale de la recherche et du développement, Service des pêches et de la mer, ministère de l'Environnement. Les numéros 715 à 924 ont été publiés à titre de Rapports techniques du Service des pêches et de la mer, ministère des Pêches et de l'Environnement. Le nom actuel de la série a été établi lors de la parution du numéro 925.

Canadian Technical Report of
Fisheries and Aquatic Sciences 3277

2018

JUVENILE SALMON ACOUSTIC MONITORING IN THE DISCOVERY ISLANDS, BRITISH COLUMBIA

By

S. Rousseau[1], S. Gauthier[2], S. Johnson[3]
C. Neville[3] and M. Trudel[4]

[1]Thalassa, 577 Braemar Ave, North Saanich, BC, Canada, V8L 5G5
shani@thalassamarineresearch.com

[2]Fisheries and Oceans Canada, Science Branch, Pacific Region, 9860 West Saanich Road, Sidney, BC, Canada, V8L 4B2
stephane.gauthier@dfo-mpo.gc.ca

[3]Fisheries and Oceans Canada, Science Branch, Pacific Region, 3190 Hammond Road, Nanaimo, BC, Canada, V9T 6N7
stewart.johnson@dfo-mpo.gc.ca
chrys.neville@dfo-mpo.gc.ca

[4]Fisheries and Oceans Canada, Science Branch, Atlantic Region, 531 Brandy Cove Road, St. Andrews, New Brunswick, Canada, E5B 2L9
marc.trudel@dfo-mpo.gc.ca

Cat. No. Fs97-6/3277E-PDF ISBN 978-0-660-28181-0 ISSN 1488-5379

Correct citation for this publication:

Rousseau, S., Gauthier, S., Johnson, S., Neville, C. and Trudel M., 2018. Juvenile salmon acoustic monitoring in the Discovery Islands, British Columbia. Can. Tech. Rep. Fish. Aquat. Sci. 3277: viii + 31 p.

Contents

List of Figures

List of Tables

Abstract

Rousseau, S., Gauthier, S., Johnson, S., Neville, C. and Trudel, M. 2018. Juvenile salmon acoustic monitoring in the Discovery Islands, British Columbia. Can. Tech. Rep. Fish. Aquat. Sci. 3277: viii + 3 p.

This report presents the latest results of an ongoing juvenile Pacific salmon acoustic monitoring program taking place in the Discovery Islands region, between Vancouver Island and the Sunshine coast, since 2015. The project aims at improving our understanding of juvenile Pacific salmon migration dynamics and the ecological interactions between wild and farmed salmon, and is used as a pilot study to assess the use of fixed, autonomous echosounders (AZFP) for long-term monitoring of juvenile salmon abundance and distribution. These echosounders were deployed in the Discovery Islands and Johnstone Strait region during the juvenile salmon migration season in 2015, 2016 and 2017. Purse seining and a high-resolution, side-scan sonar (DIDSON) were used as a basis for comparison and validation of the acoustic data. Results show that the data obtained from the fixed echo-sounders provided an accurate representation of the migration timing and dynamics of the juvenile salmon population in the area. In 2016, when five echosounders were deployed throughout the Discovery Islands region, the migration timing remained mostly constant among sites. In Okisollo channel, our primary study area, the deeper sites (bottom depth of 110 and 70 m in 2016 and 2017, respectively) presented a lower juvenile salmon abundance than the primary site ($\sim$ 50 m bottom depth). A logarithmic relationship between juvenile salmon length and $\Delta\text{MVBS}_{67-125}$, the difference between the mean backscattering volume at 67 and 125 kHz, was derived from empirical acoustic and purse seine data.

Résumé

Ce rapport présente les plus récents résultats découlant d'un programme de surveillance de l'abondance et de la distribution du saumon juvénile du Pacifique dans la région des Iles Discovery, entre l'ile de Vancouver et la Sunshine Coast, depuis 2015. Le projet vise à améliorer notre compréhension de la dynamique de migration et des interactions écologiques entre le saumon juvénile du Pacifique et le saumon d'élevage. Cette étude est également utilisée comme projet-pilote afin d'évaluer l'utilisation d'échosondeurs autonomes (AZFP) et fixes dans la surveillance à long-terme de la distri-

bution et de l'abondance du saumon juvénile. Ces échosondeurs ont été déployés dans la région des Iles Discovery et du Détroit de Johnstone durant la période de migration du saumon juvénile en 2015, 2016 et 2017. Un échantillonnage à la seine et au moyen d'un sonar haute-fréquence (DIDSON) ont été utilisés pour comparer et valider les données acoustiques obtenues au moyen des échosondeurs fixes. Les résultats montrent que les données acoustiques obtenues au moyen des échosondeurs fixes fournissent une représentation juste de la période et de la dynamique de migration du saumon juvénile dans l'aire d'étude. En 2016, lorsque cinq échosondeurs furent déployés dans la région des Iles Discovery, la période de migration observée fut similaire d'un site à l'autre. Dans le canal d'Okisollo, notre aire d'étude principale, le saumon juvénile fut moins abondant aux sites situés en eau profonde (110 et 70 m de profondeur en 2016 et 2017, respectivement) comparativement au site principal ($\sim$ 50 m de profondeur). Une relation logarithmique a été établie entre la longueur moyenne des saumons juvéniles et $\Delta\text{MVBS}_{67-125}$, la différence entre la rétrodiffusion volumique moyenne à 67 et 125 kHz, à partir des données empiriques.

1 Introduction

Long-term monitoring of marine fish populations has long been conducted using standard fish sampling methods, such as trawling and purse seining. From the early 1980s to 1990s, significant improvements in hydroacoustic methods and technologies have allowed for the use of vessel-mounted echosounders to conduct large spatial surveys of fish stocks (Dickie et al., 1983, 1987; Foote et al., 1987; Johannesson and Mitson, 1983; MacLennan et al., 1990; Rose et al., 1988; Simmonds et al., 1991). Combined, trawl and acoustic methods are highly efficient to map distributions and abundances over large areas. However, they are generally restricted to a few surveys per year, and are therefore not practical when looking at temporal variability in abundances and distributions. In addition, to allow inter-annual comparability, these surveys are highly restricted in time and might miss important time-sensitive events, leading to a misunderstanding of the ecology and species interactions in the area.

Fixed echosounders have been used extensively in the study of near-surface bubbles and wave processes (Thorpe 1986, Vagle et al., 1992, Trevorrow, 2003). More recently, they have been used to study zooplankton and pelagic fish distribution and behaviour (Thomson et al., 2000; Kaartvedt et al., 2009, Sato et al., 2013). The recent development of several ocean observatories (Favali et al., 2015) have sparked an increase in the number of moored inverted echosounders deployed for long-term monitoring of pelagic communities (Pawlowvicz and McLure, 2010).

In this study, we use autonomous, inverted echosounders to study the migration timing and dynamics of juvenile salmon distribution in the Discovery Islands and Johnstone Strait, as part of a larger effort to understand the survival of juvenile salmon during their outward migration and the impacts and importance of disease transfer from aquaculture sites to the wild population. Information on the migratory pathways of wild salmon and the duration of their residency in the vicinity of fish farms, their direct interaction with farm facilities, as well as their overall physiological well-being and health are key to increasing knowledge and understanding of how aquaculture operations impact the ecosystem. This study also evaluates the use of fixed, autonomous echosounders for long-term monitoring of juvenile salmon in the area.

2 Materials and Methods

2.1 Study area and survey design

Located between the eastern side of central Vancouver Island and the British Columbia mainland, the Discovery Islands area is made of a complex network of narrow channels and deep fjords (Foreman et al., 2012). Water circulation is dominated by tides, with strong currents occurring in Johnstone Strait, while lowest tidal currents are observed southeast of Quadra Island and in Kanish and Waiatt Bay in the north (Figure 1).

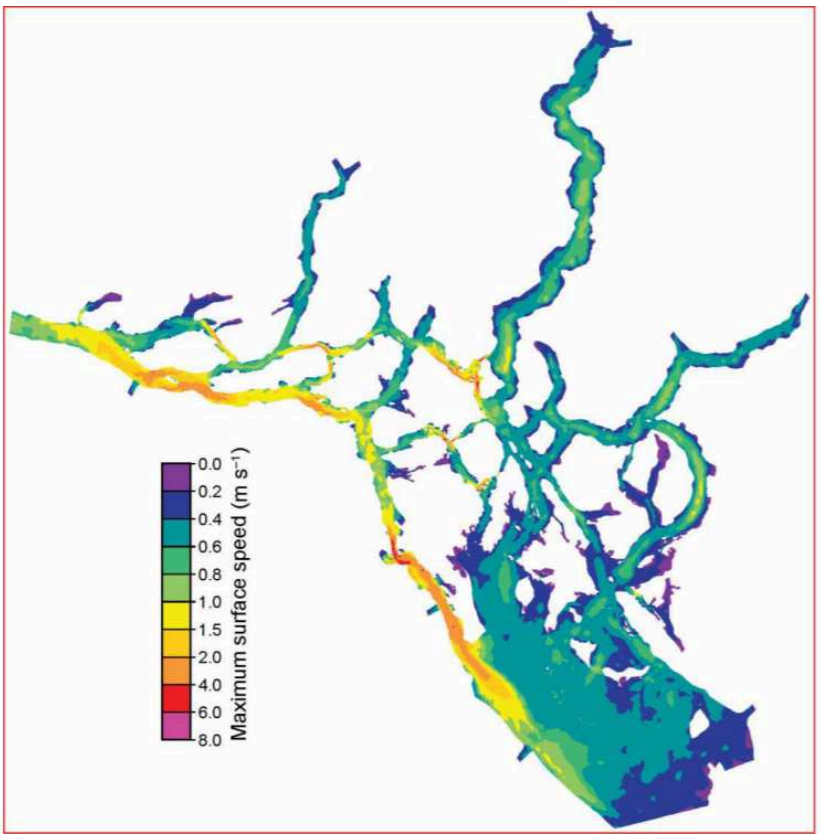

Figure 1: Maximum surface speeds (ms^{-1}) over a 28-day model simulation period (April 1- 28 2010) (Foreman et al., 2012).

Moored inverted echosounders were deployed at several locations in the Discovery Islands and Johnstone Strait area in 2015, 2016 and 2017 to collect data primarily during the expected juvenile salmon migration period, which usually extends from early May to July. Four moorings were deployed in

2015, five in 2016, and two in 2017 (Figure 2). Tables 1, 2 and 3 give a summary of the data collected at each site.

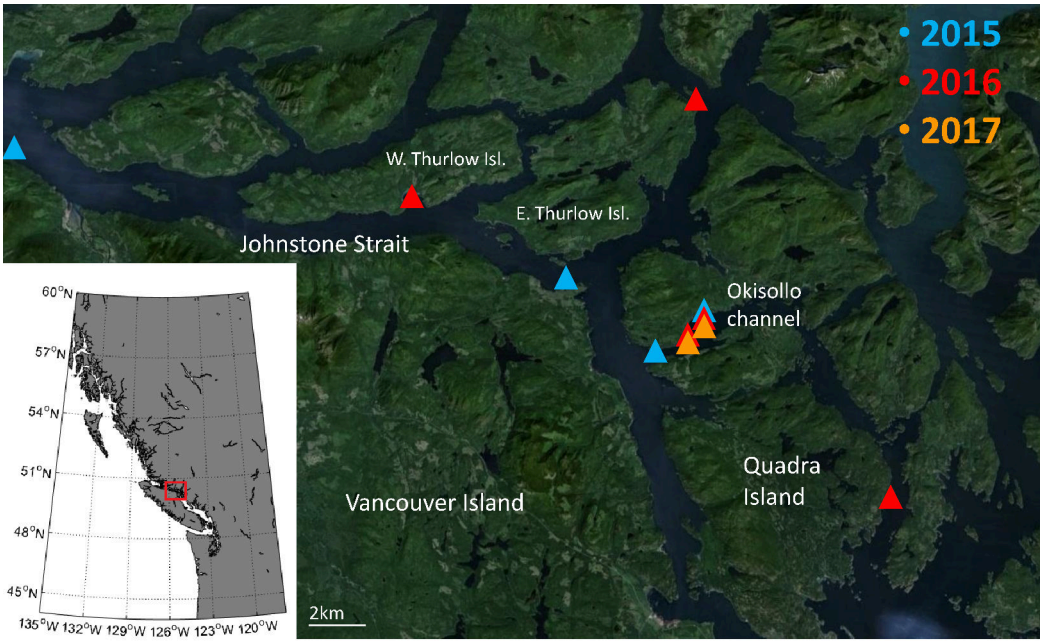

Figure 2: Mooring locations in 2015, 2016 and 2017 in the Discovery Islands and Johnstone Strait area.

The primary location used for this study was Okisollo channel, a sheltered body of water separating the islands of Sonora and Quadra in the Discovery Islands. This area is known as a juvenile salmon hotspot in May and June, and is home to several Atlantic salmon aquaculture sites (Figure 3).

The primary site (Venture Point) in Okisollo channel was located approximately 170 m from shore, in a small bay north-east of Cermaq's Venture Point aquaculture farm. The bottom depth at the mooring site varied slightly from year to year (tables 1, 2 and 3). In 2015, a second mooring was deployed near the west entrance to Okisollo channel, between Metcalf and Brent Islands. This site was located approximately 120 meters from shore and 205 meters west of Cermaq's Brent Island aquaculture farm. It was deployed at a bottom depth of 53 meters. In 2016, a second mooring was deployed 200 meters off of Venture Point, in 110 meters of water. Finally, in 2017 the second mooring deployed in Okisollo was located 345 meters south of the primary Venture Point site, 430 meters offshore and 70 meters deep.

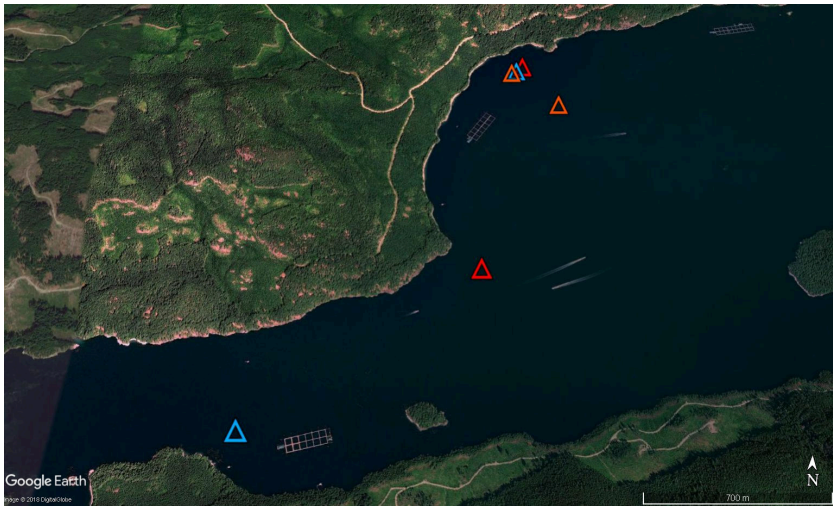

Figure 3: Okisollo channel mooring sites in 2015 (blue), 2016 (red) and 2017 (orange), with Cermaq's Brent Island and Venture Point aquaculture farms.

In 2015, two moorings were deployed in Johnstone Strait. The most western site was deployed just east of Hickey Point, 50 meters from shore in 33 meters of water (figure 4). This site was located near DFO's primary purse seining site for juvenile salmon monitoring. The second site was deployed just west of Chatam Point, 150 meters offshore in Rock Bay at a bottom depth of 43 meters (figure 5). These two sites were exposed to winds and tidal currents and presented some analytical challenges due to the presence of bubbles caused by surface waves which contaminated the acoustic signal. The signal from these bubbles is stronger than that of fish schools, greatly reducing the usefulness of the acoustic data during periods of strong winds.

In 2016, the three moorings not deployed in Okisollo channel were deployed at Channe Island, Hoskyn channel and Knox Bay. These sites cover several possible pathways for juvenile salmon migration through the Discovery Islands and are accessible by the purse seiner. These locations were also chosen in order to reduce the chance of bubble contamination.

The site deployed near Channe Island was located 93 meters from shore in Channe Passage, between Channe and East Thurlow Islands, at a bottom depth of 58 meters (figure 6). Channe passage is oriented northwest-southeast, and strong winds can sometimes form in this direction.

Knox Bay, on the south shore of West Thurlow island, is approximately 1.3 km long and wide; the mooring was located 175 meters from shore near the

Figure 4: Johnstone Strait mooring site, deployed in 2015.

Figure 5: Chatam Point mooring site, deployed in 2015.

west side of the bay, in 52 meters of water (figure 7). The bay faces south, toward Johnstone Strait.

Hoskyn channel is located east of Quadra island; the mooring was deployed in a small bay south of Conville Point, 136 meters from shore at a bottom depth of 54 meters (figure 8). The area is open to southerly winds and swell.

Figure 6: Channe Island mooring site, deployed in 2016.

Figure 7: Knox Bay mooring site, deployed in 2016.

Table 1: Summary of 2015 data collection.

Site	Location	Coordinates	AZFP serial #	Frequency (kHz)	Bottom depth (m)	Start date/time	End/date time
1	Venture Point	$\frac{50.3057° N}{125.3348° W}$	55084	$\frac{67/125}{200/455}$	55	2015-05-13	2015-09-30
2	Brent Island	$\frac{50.2861° N}{125.3538° W}$	55086	$\frac{67/125}{200/455}$	53	2015-05-14	2015-09-30
3	Chatam Point	$\frac{50.3308° N}{125.4603° W}$	55026	200	43	2015-05-14	2015-09-30
4	Johnstone Strait	$\frac{50.4392° N}{126.0537° W}$	55085	$\frac{67/125}{200/455}$	33	2015-05-15	2015-09-30

Figure 8: Hoskyn Channel mooring site, deployed in 2016.

Table 2: Summary of 2016 data collection.

Site	Location	Coordinates	AZFP serial #	Frequency (kHz)	Bottom depth (m)	Start date/time	End/date time
1	Venture Point	$\frac{50.3060^\circ N}{125.3343^\circ W}$	55086	$\frac{67/125}{200/455}$	61	2016-05-11	2016-09-15
2	Okisollo Deep	$\frac{50.2939^\circ N}{125.3377^\circ W}$	55124	67	110	2016-05-11	2016-09-28
3	Knox Bay	$\frac{50.3871^\circ N}{125.6161^\circ W}$	55085	$\frac{67/125}{200/455}$	52	2015-05-12	2015-09-17
4	Channe Island	$\frac{50.4538^\circ N}{125.3363^\circ W}$	55026	200	58	2015-05-10	2015-10-01
5	Hoskyn Channel	$\frac{50.1901^\circ N}{125.1419^\circ W}$	55084	$\frac{67/125}{200/455}$	54	2015-05-13	2015-09-22

Table 3: Summary of 2017 data collection.

Site	Location	Coordinates	AZFP serial #	Frequency (kHz)	Bottom depth (m)	Start date/time	End/date time
1	Venture Point	$\frac{50.3055^\circ N}{125.3352^\circ W}$	55086	$\frac{67/125}{200/455}$	50	2017-05-04	2017-10-07
2	Okisollo Deep	$\frac{50.3035^\circ N}{125.3315^\circ W}$	55026	200	70	2017-05-04	2017-10-08

2.2 Data collection

2.2.1 Instrument setup

Each mooring consisted of a bottom-mounted AZFP echosounder (Acoustic Zooplankton and Fish Profiler, ASL Environmental Sciences), one or two temperature and pressure sensors (RBR Ltd.) that sampled at a rate of 30 seconds, and an acoustic release (Subseasonic AR-60-E) (figure 9). Three of the AZFP echosounders operated at four frequencies (67, 125, 200, and 455 kHz); the remaining two operated at one frequency (67 or 200 kHz). In the multi-frequency units, the elements for the three higher frequencies are located within a single transducer unit; the larger 67 kHz transducer requires a single housing unit. The two transducers were located approximately 30 cm from each other over a metal frame (figure 10). Each echosounder was calibrated by the manufacturer prior to deployment and after recovery.

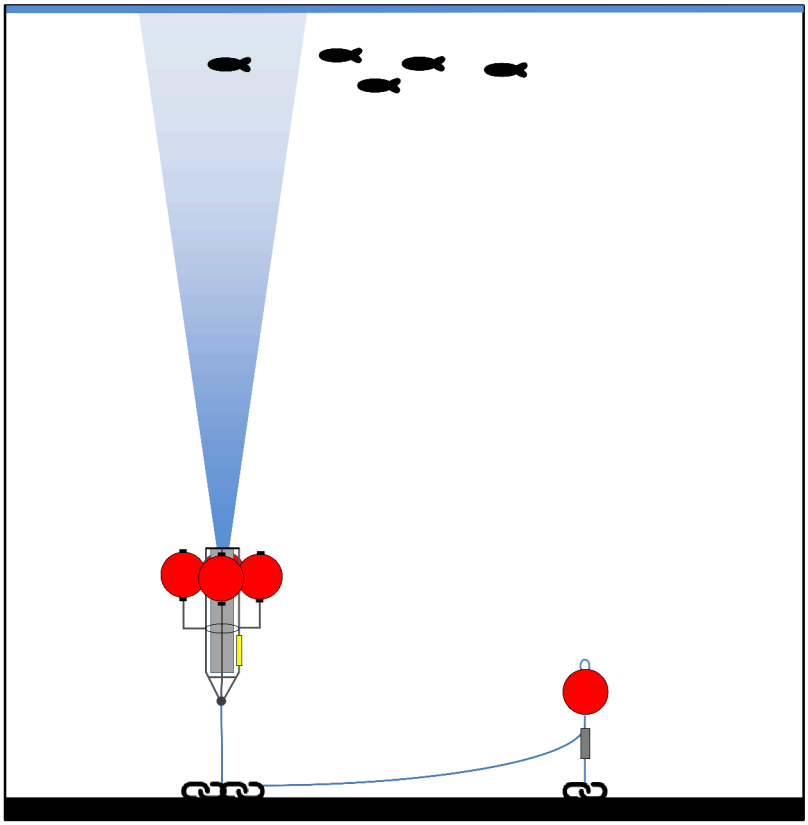

Figure 9: Mooring schematic. Image not to scale.

Figure 10: Multi-frequency AZFP echosounders (ASL Environmental Sciences) after being recovered from Okisollo channel in 2016.

The AZFP hardware can be set to operate under different parameter settings and/or ping regime during a single deployment. Each setting is called a phase. Table 4 describes the sampling rate used for each station and phase. The sampling rates were chosen as to maximize data resolution during expected high juvenile salmon presence (May to July) but was limited by battery consumption and memory usage. A pulse duration of 500 μs was used at 67 kHz, and 300 μs was used at 125, 200 and 455 kHz. A digitization rate of 64 kHz was used for all frequencies.

Table 4: Sampling rates used at each site and phase in 2015, 2016 and 2017. Phase 1: Start of recording to August 01. Phase 2: August 01 to end of recording.

Site	1		2		3		4		5	
Phase	1	2	1	2	1	2	1	2	1	2
Year										
2015	3	5	3	5	1	NA	3	5	NA	
2016	3	5	2	4	3	5	1	2	3	5
2017	3	NA	2	3	NA		NA		NA	

In order to resolve single acoustic targets from the received echo, the range difference between target 1 and target 2 must be large enough for the two echoes not to overlap (Simmonds and MacLennan, 2005):

$$R_2 - R_1 = \frac{c\tau}{2} \tag{1}$$

where c is the speed of sound in seawater ($\sim$ 1500 ms^{-1}) and τ is the pulse duration (s). R_1 and R_2 represent the ranges to target 1 and target 2. Given a pulse duration of 500μs at 67 kHz and 300μs at 125, 200 and

455 kHz, the minimum single target resolution distance is 37.5 cm and 22.5 cm, respectively. Below this distance, single targets are not resolved, and the targets show as aggregations. The corresponding acoustic signal is calculated as the sum of all signals divided by the sampling volume.

2.2.2 CTD casts

CTD casts were collected throughout the summers of 2015, 2016 and 2017 in the area of study by various DFO sampling programs as well as the Hakai Institute. These casts were used to determine the monthly average profile of sound speed and absorption coefficient at each station to be used in the post-processing stages of acoustic data analysis.

2.2.3 Purse seine

Purse seine surveys were conducted twice a week by Fisheries and Oceans Canada from May 12 to July 15 in 2015 and from May 17 to July 13 in 2016. In 2017, purse seine data was collected in Okisollo channel every few hours for a period of 24 hours on June 14, July 12 and September 12, to study the changes in fish composition over an entire daily cycle and help with the validation of the acoustic data. Sampling was performed with a small mesh purse seine on a commercial seiner during slack and low flow tides to ensure that the net opening remained stable during fishing operations and that catch-per-unit-effort (CPUE) was comparable among sampling events.

2.2.4 DIDSON

Short acoustic surveys using a vessel-mounted, side-looking sonar (DIDSON) were conducted above and around all mooring sites in June and July of 2015 and 2016. The DIDSON is a low-range, high resolution sonar, which allows detection of near surface targets such as juvenile salmon. Along-shore transects at increasing distance from the shoreline were conducted to provide information on the fine-scale spatial dynamics in the area of the moorings. This data was also compared to the bottom-mounted acoustic data to improve certainty in target identification. The DIDSON software (v5.26.06) was used for fish counting.

2.3 Data analysis

2.3.1 Computation of Sv and TS

All acoustic analyses were performed with Myriax Echoview (version 8.0), R (version 3.3.1) and Matlab (version 8.5). For the AZFP, the mean volume backscattering strength (S_v) and the target strength (TS) are calculated as follows:

$$TS = EL_{max} - \frac{2.5}{a} + \frac{N}{26214a} - TVR - 20logV_{TX} + 40logR + 2\alpha R \quad (2)$$

$$S_v = EL_{max} - \frac{2.5}{a} + \frac{N}{26214a} - TVR - 20logV_{TX} + 20logR + 2\alpha R - 10log(\frac{c\tau\psi}{2}) \quad (3)$$

where EL_{max} is the echo level (in dB re 1 μPa) at the transducer that produces full-scale output; N, in counts, is the digital recorded value and is linearly related to the received voltage (v_{in}) after it has been amplified, bandpass filtered, and passed through a so-called "detector" whose output is a function of $\log(v_{in}^2)$; a is the slope of the detector response; TVR is the transmit voltage response of the transducer in dB re 1 μPa/volt at 1 m range; V_{TX} is the voltage amplification factor before it is sent out; α is the absorption coefficient; c is the sound speed; and τ is the pulse length. R is the range calculated as $R = ct/2$. $40logR + 2\alpha R$ and $20logR + 2\alpha R$, in equations 2 and 3, respectively, represent the time-varied-gain (TVG) applied to compensate for transmission loss (TL). ψ, the equivalent-beam-angle, is approximated by

$$\psi = 1.4\pi(1 - cos\theta) \quad (4)$$

where θ is half the full -3 dB beam angle of the transducer. For more information on the conversion from voltage to acoustic signal specific to the AZFP, please refer to ASL Environmental's AZFP Operator's Manual.

The echograms were treated in their original, reversed perspective with the tidal amplitude evident at the top (figure 11). This method allowed for easier correction of range-dependent noise issues such as side-lobe and TVG. The depth was estimated as an offset from the detected surface.

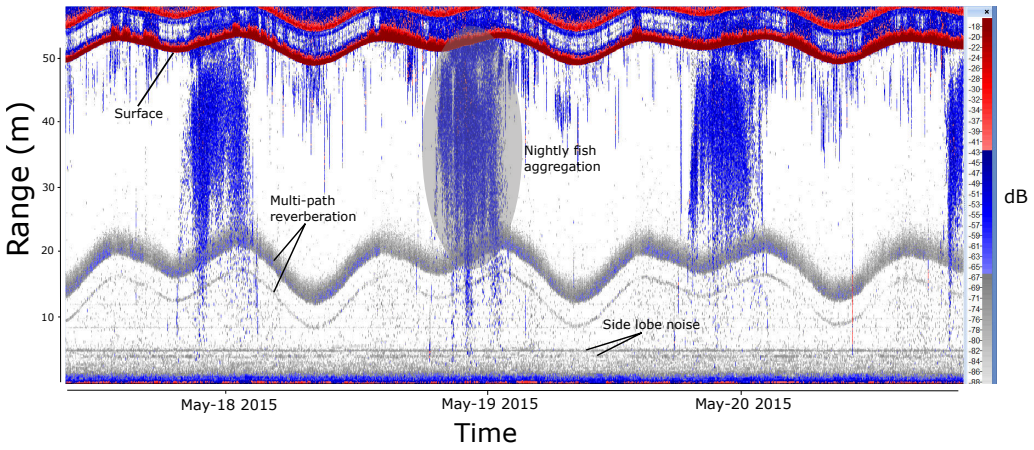

Figure 11: Example of a typical echogram showing surface backscatter (with tidal pattern visible) and large nightly aggregations (shaded). Multi-path reverberation and side lobe noise are also indicated.

2.3.2 Defining the surface and removing bubble noise

Echoview's *best bottom candidate* algorithm was used to detect and define backscatter from the surface. Echoview's default parameters were used. The resulting line was smoothed to exclude higher frequency variations caused by waves and other strong signals such as fish schools, using a 49 pings (maximum window permitted by the Echoview operator) running window filter selecting the maximum detected range (shallowest depth) within that interval. The resulting line was reviewed manually and used as the surface reference.

Bubbles originating from surface waves were sometimes found to contaminate the acoustic data near the surface. In particular, deep bubble entrainment generated acoustic noise down to depths of 20 m at the Johnstone Strait and Chatam Point sites in 2015. Consequently, in 2016 care was taken to ensure that moorings were deployed in regions of minimal wind-generated waves. However, it was not possible to completely avoid bubble noise near the surface. To exclude this signal from the analysis, an exclusion line was generated from the 125 kHz data using Echoview's *Maximum Sv* algorithm (discrimination level of -80 dB with -0.3 m backstep). Data at 125 kHz were used because the acoustic signal from bubbles is often stronger at this frequency (Trevorrow et al., 1993). The exclusion line was reviewed and corrected manually when fish schools at the surface were mistakenly selected as surface waves. To help separate bubbles from fish signals during the manual correction, the difference between the 67 and 125 kHz frequencies (ΔMVBS)

was used. Whereas the acoustic signal from fish is fairly stable across frequencies, bubbles backscattering properties are frequency-dependent (Benoit-Bird and Lawson, 2016).

An offset of 0.3 m was applied to the final line delineating the lower limit of bubble noise (figure 12). Data above this line, as well as data below a 5 m distance from the transducers' face, where side lobes had more effects, were excluded from the analysis.

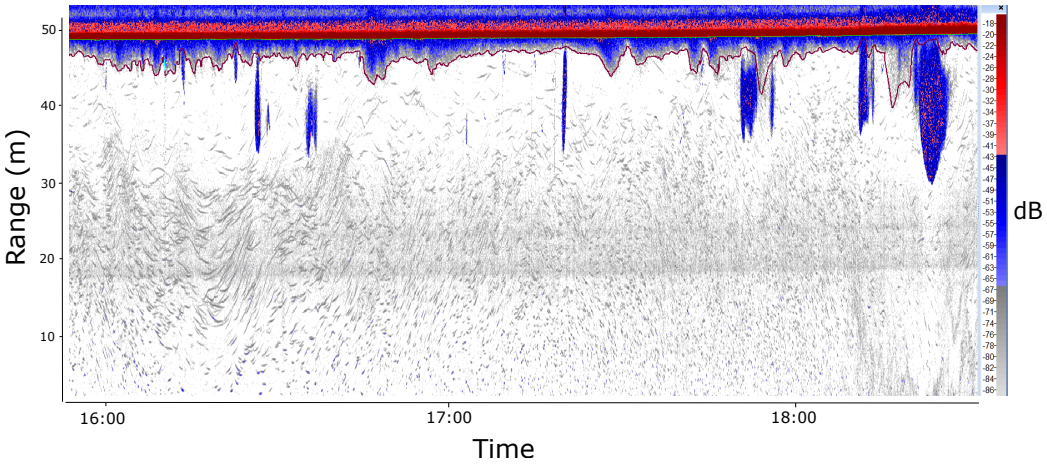

Figure 12: Example of a typical echogram showing the line (purple) defining bubbles near the surface. Example taken from the site 2 time series on May 25 2015.

2.3.3 Background noise removal

Background noise was removed by linear subtraction using Echoview's *Background Noise Removal* algorithm (DeRobertis and Higginbottom, 2007). Thresholds for maximum estimated noise were -125 dB at 67, 125 and 200 kHz, and -110 dB at 455 kHz and were determined empirically. A signal-to-noise ratio of 10 dB specified the acceptable limit for a signal to be deemed distinguishable from noise.

2.3.4 School detection and classification

Fish schools were detected using Echoview's school detection module (Barange, 1994, Coetzee, 2000). Table 5 shows the selection parameters for school detection. Note that Echoview requires GPS input in order to run the school detection algorithm. For this study, we converted the time units into distance by creating an imaginary GPS linear track of 1 knot (0.51 m/s). The 67 kHz

Table 5: Parameters used for the school detection. Note that values were converted from the time domain to distance units to be compatible with Echoview's school detection algorithm.

Parameters	Value
Minimum threshold (dB re m^{-1})	67
Minimum total school length (s)	24
Minimum total school height (m)	1
Minimum candidate length (s)	20
Minimum candidate height (m)	1
Maximum vertical linking distance (m)	2
Maximum horizontal linking distance (s)	20

echogram was smoothed (20 samples x 9 pings mean in the linear domain) and a -67 dB threshold applied prior to running the module. This threshold was chosen in order to include as much of the signal from fish as possible, while excluding noise from the second surface echo. The resulting smoothed and thresholded echogram was only used to define the perimeter of the fish schools, not to export the acoustic variables.

Echoview's region classification module was used to separate the detected schools into categories, which were further inspected visually. Here, we focus on two school categories: near-surface schools were ascribed to juvenile salmon based on purse seine, visual surveys, and DIDSON data collection. In 2015, juvenile salmon prevailed by 90% over herring in 31 out of 36 purse seine samples collected. This number increased to 100% in 2016. Deeper, elongated schools with higher acoustic densities were consistent with herring (figure 13).

2.3.5 Computation of NASC and fish density

The density of fish per unit area (ρ_a) is defined as:

$$\rho_a = \frac{NASC}{4\pi \times \sigma_{bs}} \tag{5}$$

where σ_{bs} is the backscattering cross section (m^2):

$$\sigma_{bs} = 10^{\frac{TS}{10}} \tag{6}$$

The target strength (TS) is constant for a fish target of the same species and size. NASC, the nautical area scattering coefficient ($m^2 nmi^{-2}$) is a measure of acoustic signal per surface area:

$$NASC = 4\pi \times 1852^2 \times 10^{\frac{S_v}{10}} \times T \tag{7}$$

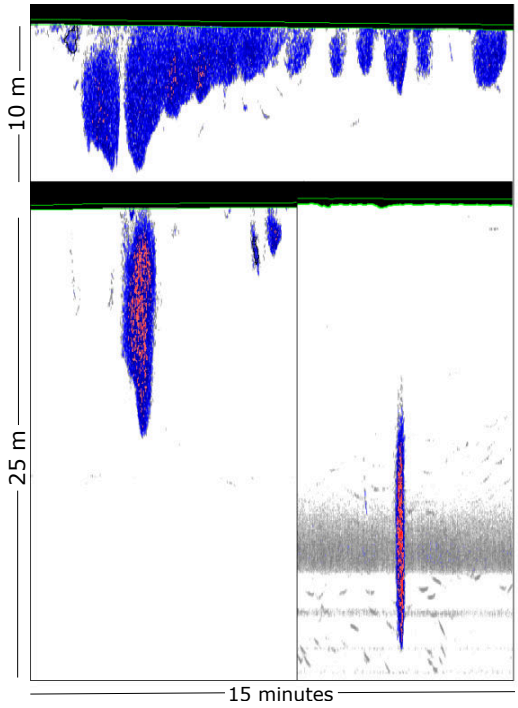

Figure 13: Example of a typical acoustic signal for juvenile salmon (upper panel) and herring schools (lower panel).

where T is the thickness (vertical extent) of the analysis domain and S_v the mean volume backscattering strength. Here, we use the entire water column contained in the analysis domain as T. The Elementary Time Sampling Unit, or ETSU, is defined as the length of time on which the acoustic measurements are averaged to give one sample. In this study, we use 1 day (excluding time between sunset and sunrise) as ETSU unit to explore seasonal variations in NASC, and we use 1 hour as ETSU unit to explore relationships between NASC and daily cycles such as tides and light.

In this study, the TS value for juvenile salmon is unknown; thus we use NASC as a proxy for fish density, since they are linearly proportional - assuming homogeneous schools of identical species and similar size, and a random distribution of fish within the beam (Parker-Stetter et al., 2009).

2.3.6 Difference in mean backscattering volume

The difference in mean backscattering volume (ΔMVBS) between one or more frequency pairs is commonly used to separate acoustic scatterers into categories. The efficacy of this method varies; it has been used successfully

to distinguish zooplankton from other scatterers like fish because the echoes from plankton are more highly dependent on frequency than the echoes from fish (Lavery et al., 2007). A number of studies also discuss the potential of using this method to differentiate between species of fish (DeRobertis et al., 2010; Sato et al., 2015). Here, we use this method as a post-classification validation method for the choice of our two main classes (Juvenile salmon and Herring), and to develop a relationship between mean fish length and ΔMVBS.

Acoustic backscatter differences for all possible frequency pairs (67, 125 and 200 kHz) were calculated for each averaged cell (30 seconds x 0.5 m mean in linear domain) of the S_v analysis domain. The 455 kHz frequency was excluded from this analysis because the signal-to-noise ratio decreased too rapidly with range at this frequency to allow for an accurate comparison with the other frequencies.

A difference in backscatter in the logarithmic domain is equivalent to its ratio in the linear domain:

$$S_{vf_2} - S_{vf_1} = s_{vf_2}/s_{vf_1} \tag{8}$$

where $S_v = 10log_{10}(s_v)$, and s_v is the volume backscattering coefficient (m^{-1}, MacLennan et al., 2002).

To minimize the effects of background noise, only cells where the mean backscattering volume (MVBS) was greater than -70 dB for at least one of the frequencies in the pair were used for further analysis.

2.3.7 Relationship between standard length and acoustic signal

Target strength (TS) is related to fish length as follows (Simmonds and MacLennan, 2005):

$$TS = a\log_{10}(L) + b \tag{9}$$

The target strength for an individual fish target is defined as

$$TS = 10\log_{10}(\sigma_{bs}) \tag{10}$$

where σ_{bs} is the backscattering cross-section (m^2). Combining equations 9 and 10 yields

$$10 \log_{10}(\sigma_{bs}) = a \log_{10}(L) + b \tag{11}$$

σ_{bs} can also be expressed in terms of s_v, the volume backscattering coefficient (m^2 m^{-3}):

$$s_v = \frac{\sum_{n=1}^{N} \sigma_{bs}}{V} \tag{12}$$

where N is the total number of fish and V the sampling volume. Assuming that all fish in the sampling volume have a similar length, equation 12 becomes

$$s_v = \frac{N\sigma_{bs}}{V} \tag{13}$$

This assumption is true only if the observed schools are composed of individuals of same species and similar size.

S_v, the volume backscattering strength, is defined as the logarithmic transformation of s_v (dB re: 1 m^{-1}):

$$S_v = 10 \log_{10}(s_v) \tag{14}$$

Combining equation 14 with equation 11, we obtain a relationship between $\Delta MVBS_{67-125}$, the difference in mean volume backscattering strength at 67 and 125 kHz, and the mean fish length within the sampling volume:

$$\Delta MVBS = S_{v2} - S_{v1} = c \log_{10}(L) + d \tag{15}$$

Where c and d are respectively the slope and the intercept of the model. This equation was used to determine the relationship between $\Delta\text{MVBS}_{67-125kHz}$ and the standard length of juvenile salmon using the empirical acoustic data from the Venture Point site and the fish length data collected in Okisollo channel.

3 Results and discussion

3.1 Backscatter from wave generated bubbles

Several sites presented a high concentration of air bubbles near the surface which prevented the acoustic detection of juvenile salmon. Table 6 shows the percentage of backscatter that was not contaminated by air bubbles below 2 meters in 2015, 2016 and 2017. The Johnstone Strait site in 2015 presented

the highest level of bubble-generated acoustic noise, with only 38 % of the data not contaminated with air bubbles below 2 meters. That same year, sites at Chatam Point and Brent Island also presented significant amounts of bubble-generated acoustic noise. The primary site in Okisollo channel (Venture Point) was mostly noise-free (> 90 %).

Table 6: Percentage of data where backscatter from bubbles extended to less than 2 m deep under the surface. Calculated on 15 min average.

Site	% good data
2015	
Venture Point	95
Brent Island	77
Johnstone Strait	38
Chatam Point	62
2016	
Venture Point	94
Venture Point (deep)	96
Knox Bay	82
Hoskyn Channel	85
Channe Island	91
2017	
Venture Point	98
Venture Point (deep)	94

We obtained a good correlation between the occurrence of bubbles in the surface acoustic data and winds as measured by various Fisheries and Oceans Canada and Environment Canada weather stations. Figure 14 shows the time series of winds and the depth of air bubbles when wind data were available. This helps to confirm that our method for identifying bubbles backscatter near the surface is valid.

3.2 Distribution and migration timing of juvenile salmon

Figure 15 shows the acoustic abundance index at the Venture Point site in Okisollo channel, and the juvenile salmon catch (main species) obtained by the purse seiner in the same area in 2015, 2016 and 2017. The migration timing obtained from the two datasets were well correlated: in 2015, the migration timing was detected from mid-May to mid-July, whereas it was

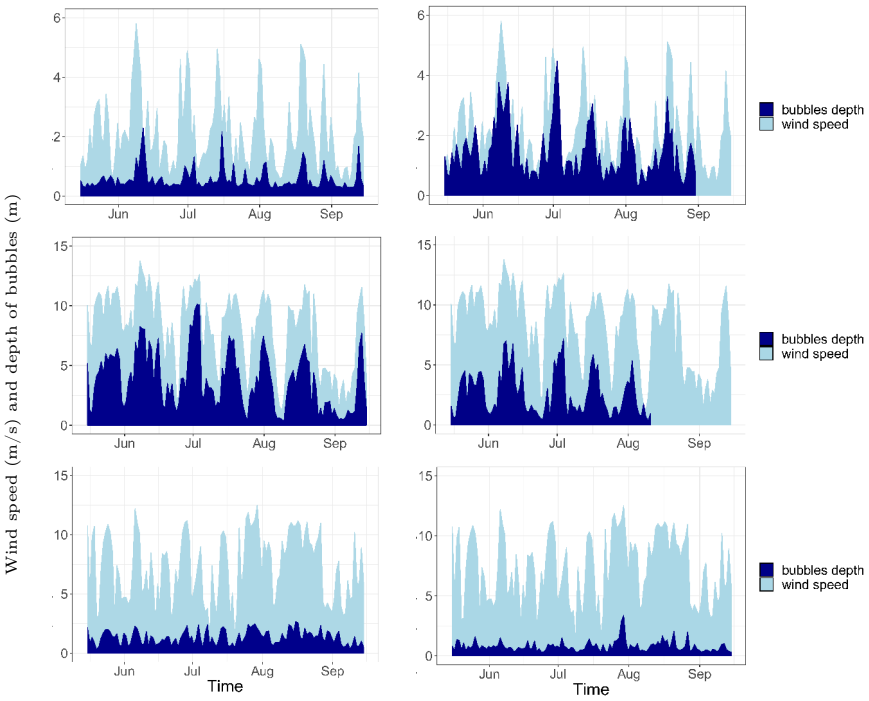

Figure 14: Time series of depth of bubbles and wind speed. A) 2015 Venture Point; B) 2015 Brent Island; C) 2015 Johnstone Strait; D) 2015 Chatam Point; E) 2016 Knox Bay; F) 2016 Channe Island. Wind data for Venture point and Brent Island in 2015 come from the Venture Point weather station (Fisheries and Oceans Canada); other wind data come from the Fanny Island weather station (Environment Canada).

detected from mid-May to mid-June in 2016. In 2017, the migration timing was detected acoustically from early June to the end of July.

The purse seine data suggest that in 2015 and 2017, the juvenile salmon population passing through Okisollo channel was dominated by sockeye (*Oncorhynchus nerka*) and chum (*Oncorhynchus keta*). During those years, the acoustic data show variable abundance throughout the migration period, whereas the migration period was short and the abundance consistently high in 2016, a year dominated by sockeye only. The purse seine data also show that chum migrated later and were slightly bigger (1-2 cm) than sockeye as they migrated through this region. In 2017, the migration period was delayed by almost 2 weeks relative to the two previous years, according to the acoustic data. This delay was confirmed by other groups studying juvenile salmon migration in the area (per. comm. 2018, Brett Johnson, Hakai Institute; Kintama, 2018), and is supported by the 2017 DIDSON data.

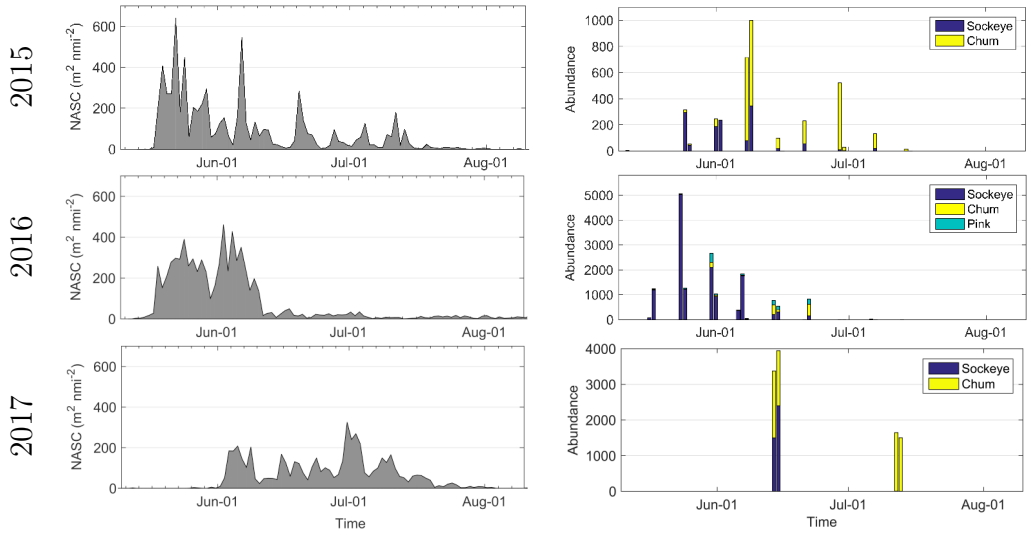

Figure 15: Left panel: Acoustic abundance index at the Venture Point site. Right panel: Juvenile salmon catch as obtained from the purse seiner in Okisollo channel. Month label indicates first day of the month.

In 2015, comparison of the two sites sampled in Okisollo channel (Venture Point and Brent Island) shows comparable migration period and timing, as well as a similar trend in temporal variability (figure 16).

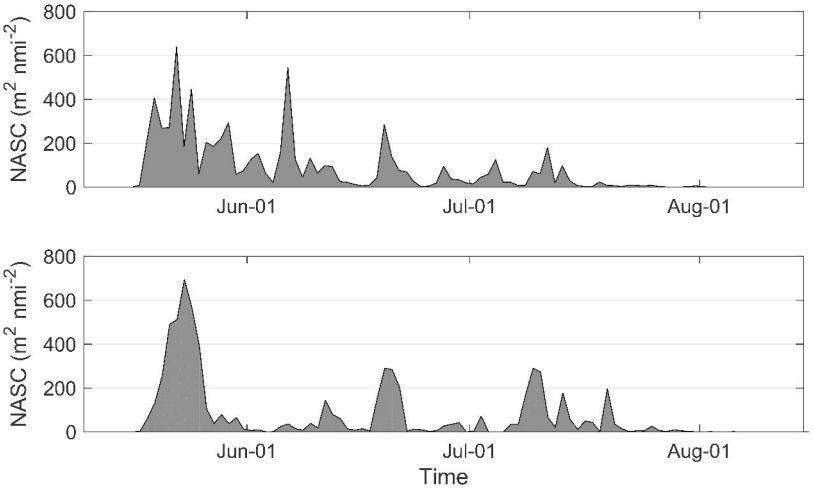

Figure 16: Acoustic abundance index at Venture Point (upper panel) and Brent Island (lower panel) sites in 2015.

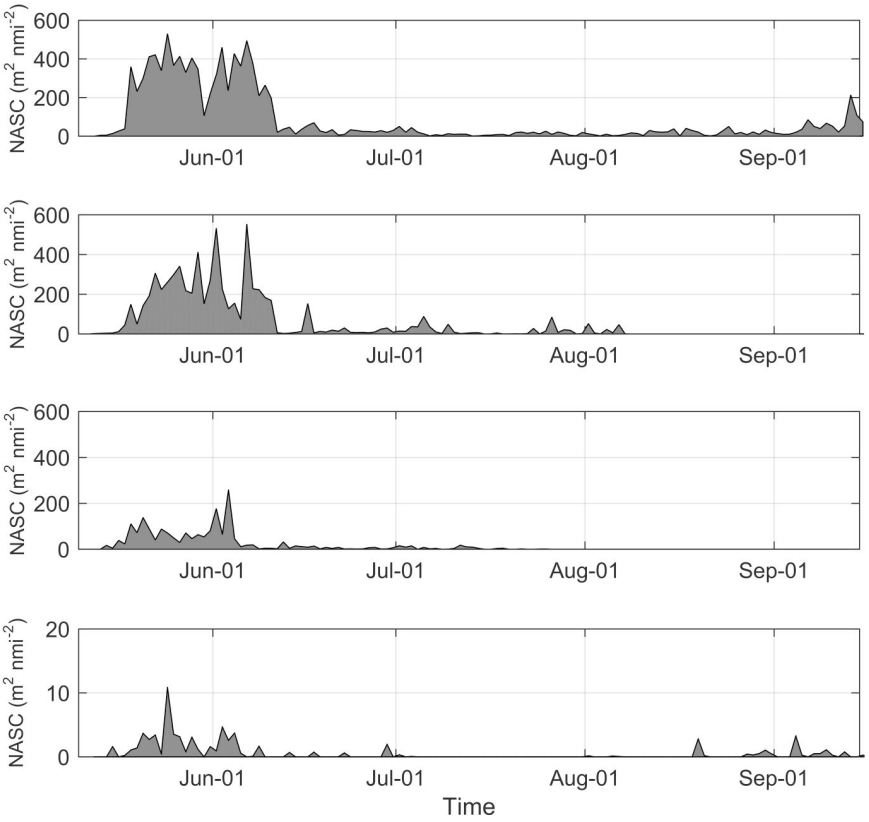

Figure 17: Acoustic abundance index at (from top to bottom) Venture Point, Okisollo Deep, Knox Bay and Channe Island sites in 2016. Note the different y-scale used for Channe Island. The acoustic data displayed were collected at 67 kHz at all sites except Channe Island, where they were collected at 200 kHz.

In 2016, analysis of the remaining mooring stations revealed variable dynamics in terms of juvenile salmon abundance, while the timing period was consistent throughout the area (figure 17). The Knox Bay site (south of West Thurlow Island) presented a lower abundance relative to the Okisollo channel sites (Venture Point and Okisollo Deep), and the Channe Island site (north-east of East Thurlow Island) presented a negligible abundance of juvenile salmon. The acoustic data at the Hoskyn channel site, east of Quadra Island, differed significantly from the other sites. In this area, we did not regularly observe the typical juvenile salmon formations near the surface, but instead we sometimes observed a dense near-surface layer, as well as numerous targets and small schools in the mid-water. This suggests that this may have been an area of transition (both in terms of behavior and movement) for juvenile salmon residing in the Strait of Georgia and those migrating through

the Discovery Passage. Unfortunately the DFO purse seine program did not sample in this area, which complicates the data interpretation at this site. For these reasons it is not included in this report.

3.3 Abundance of juvenile salmon in relation to water depth and distance from shore

In 2016 and 2017, a mooring was deployed not far from the Venture Point site in Okisollo channel but at a greater depth, to study variations in juvenile salmon abundance in relation to water depth and distance from shore. In 2016, the mooring was deployed at a bottom depth of 110 m, in a dynamic area 200 meters off of Venture Point, 1300 m south of the primary Venture Point site. In 2017, the mooring was deployed at a depth of 70 m, 430 m from shore and 345 m away from the primary Venture Point site. The juvenile salmon abundance indices at the deep and shallow sites were similar in 2016 (figure 18); in 2017, however, they were much lower at the offshore/deeper site. The two deep sites sampled in 2016 and 2017 are largely different in terms of water depth, bathymetry and current dynamics. This could affect a number of factors that might lead juvenile salmon to favour one area over another, such as prey availability and predator avoidance.

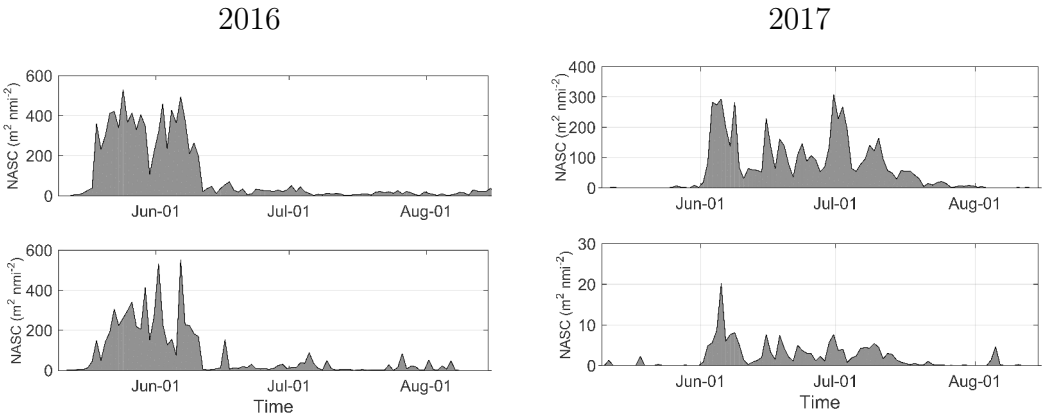

Figure 18: Acoustic abundance index at Venture Point (upper panel) and Venture Point deep (lower panel) sites in 2016 and 2017. Note the different y-scale for the deep site in 2017. The acoustic data displayed were collected at 67 kHz in 2016 and at 200 kHz in 2017.

3.4 Relationship between standard length and acoustic signal

A relationship between $\Delta\text{MVBS}_{67-125kHz}$ (the difference between the acoustic signal at 67 and 125 kHz) and the standard length of juvenile salmon was developed using the empirical acoustic data from the Venture Point site and the fish length data collected in Okisollo channel (figure 19).

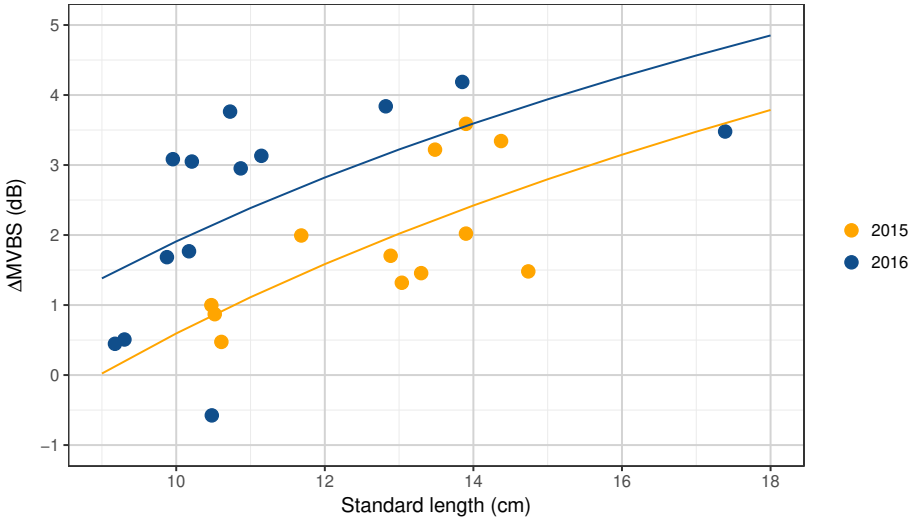

Figure 19: Relationship between $\Delta\text{MVBS}_{67-125kHz}$, the difference between the acoustic signal at 67 and 125 kHz, and the standard length of juvenile salmon collected by the purse seiner in 2016 and 2017.

The inter-annual variation observed between the years of 2015 and 2016 is likely due, at least partially, to a difference in dominant species between the years (mix of sockeye and chum in 2015, sockeye in 2016). When chum were observed in 2015, they were usually 1-2 cm larger than sockeye. This adds uncertainty to the ΔMVBS to SL relationship because it is not currently possible to differentiate these two salmon species acoustically. In 2016, the salmon population was dominated by sockeye smolts of similar size, but the salmon migration period was very short. As a result, the range of standard lengths obtained as the juvenile salmon migrated through the area was very narrow that year, thus adding to the uncertainty of the 2016 equation.

3.5 Diel variation in fish composition

On June 14-15, July 12-13 and September 12-13 of 2017, purse seine samples were collected every few hours in Okisollo channel for a period of 24 hours. Figure 20 combines all three sampling episodes to show the catch of juvenile salmon (all species combined) and herring in relation to the time of day. Juvenile salmon were caught at all times of day, with a slightly higher abundance at dawn and a lower abundance in the evening. Herring were caught mainly at dawn and dusk, during their upward and downward diel vertical migration. Chum and sockeye were the main species caught in June, whereas chum constituted most of the catch in July. Herring dominated the catch in September (table 7).

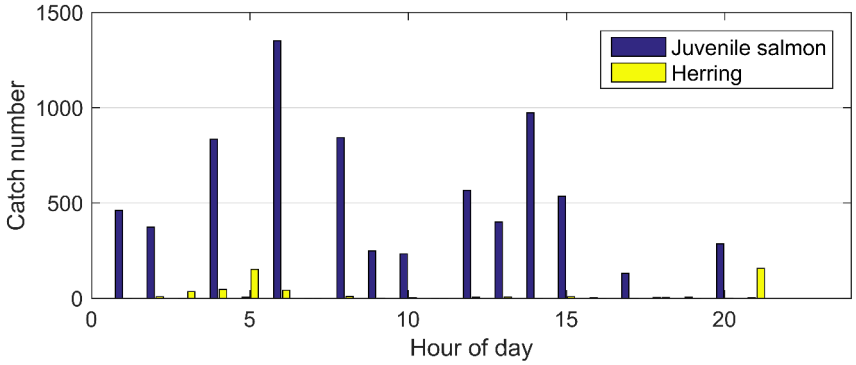

Figure 20: Proportion of salmon and herring caught by the purse seiner during the 24 hour fishing experiments conducted in June, July and September 2017.

Table 7: Purse seine catch for the main species caught during the three 24-hour sampling periods in Okisollo channel in 2017. Other fish species included pink, coho and chinook salmon, as well as sand lance. Those species all contributed to less than 0.01% of the total catch. Six, nine and eight sets were carried out on June 14-15, July 12-13 and September 12-13, respectively.

	Abundance		
Date	Sockeye	Chum	Herring
June 14-15	3897	3423	227
July 12-13	6	3144	6
September 12-13	0	33	507

Figures 21 and 22 show the 24-hour time series of the juvenile salmon catch data (all species combined), and the juvenile salmon abundance index

(NASC) as obtained from the acoustic data at the Venture Point site (bottom depth of 50 m) and the Okisollo Deep site (bottom depth of 70 m) in June and July 2017. A 24-hour time-series was also collected in September 2017, but no juvenile salmon were detected acoustically during this period, and only 42 individuals (none of them being sockeye) were collected by the purse seiner.

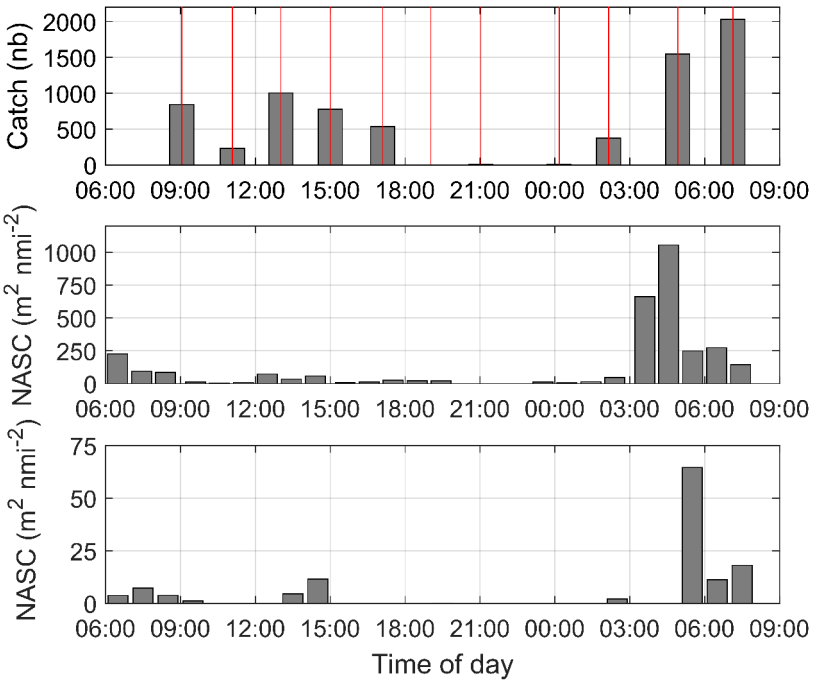

Figure 21: Purse seine catch (upper panel) and nautical area scattering coefficient of juvenile salmon at the Venture Point (middle panel) and Okisollo Deep (lower panel) sites in June 2017. Red lines in upper panel correspond to times of purse seining activity.

The June data show that the three samples collected at the beginning of the night (19h02, 21h02, 24h10) contained a very low abundance of juvenile salmon (1, 8 and 5, respectively). The acoustic data also suggest low abundances of juvenile salmon during those hours. The period of highest abundance was observed from 02h00 to 07h00 in the purse seine and in the acoustic data at both sites.

In July, a correlation between the abundance of juvenile salmon (mainly chum) and the time of day was not evident from the purse seine data. Acoustic densities were lower during this month, and a decrease was observed between 00:00 and 03:00.

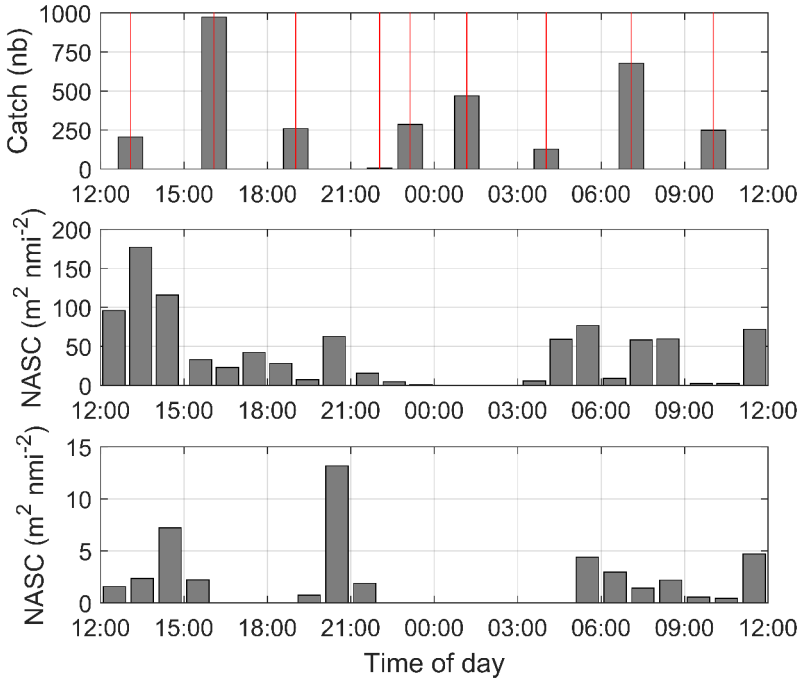

Figure 22: Purse seine catch (upper panel) and nautical area scattering coefficient of juvenile salmon at the Venture Point (middle panel) and Okisollo Deep (lower panel) sites in July 2017. Red lines in upper panel correspond to times of purse seining activity.

It is possible that, in July, when the juvenile salmon population was dominated by chum instead of sockeye, the juvenile salmon acoustic signal at night was missed if the aggregations exhibited a behaviour that was too different from their daytime behaviour - for example, if they were spread over a greater depth range, a behaviour easily confounded with herring.

The 24-hour pattern of juvenile salmon was generally similar between the two mooring sites in both June and July; however, the abundance index at the deeper site was lower by an order of magnitude. We verified whether this difference might be caused by a weaker backscattering of the juvenile salmon at 200 kHz, the frequency at which the acoustic data were collected at the deeper site. At the Venture Point site, the acoustic data were collected at both 67 and 200 kHz, and the resulting abundance index was comparable at both frequencies. Thus this difference cannot be explained by the use of a different frequency.

Figure 23 also shows the relationship between purse seine catch and the acoustic abundance index for juvenile salmon. The correlation is more evident in June ($R_{spearman} = 0.62$) than in July ($R_{spearman} = 0.21$).

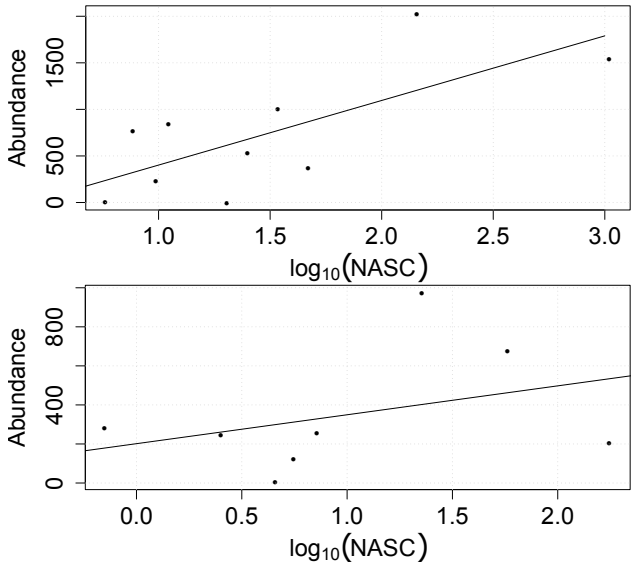

Figure 23: Logarithmic relationship between juvenile salmon purse seine catch and nautical area scattering coefficient in June (upper panel) and July (lower panel) 2017 at the Venture Point site.

4 Conclusion

This report provides an update and summary of the ongoing juvenile salmon acoustic monitoring program taking place in the Discovery Islands. Combined with findings by other programs, this study improves our understanding of the juvenile salmon distribution, migration timing, abundance and interactions with aquaculture sites in the Discovery Islands. It provides information on the level and duration of exposure of the juvenile salmon population to potential disease transfer from aquaculture sites.

The use of fixed, autonomous echosounders provides a cost-efficient, non-invasive means of monitoring juvenile salmon in the area. This three year time-series shows year-to-year variations in juvenile salmon distribution, migration timing and abundance, and their interactions with other species such as herring. It provides high temporal resolution of juvenile salmon presence as well as information on their vertical distribution (Rousseau et al., 2017). A relationship between the frequency response of juvenile salmon and

their average length was established using empirical acoustic and fish length data from Okisollo channel, allowing us to estimate juvenile salmon average length acoustically; although the uncertainties associated with this estimate are currently high.

Comparison of the juvenile salmon migration timing at the Venture Point site with other areas as well as other programs suggest that the results obtained at this site are representative of the migration timing in the Discovery Islands region. This study also demonstrates the temporal and spatial patchiness of juvenile salmon distribution and outlines the need for comprehensive sampling methods in order to get an accurate representation of the ecological dynamics in the area.

5 Acknowledgements

We gratefully acknowledge all those who contributed to this project. George Conkrite, Chelsea Stanley, Svein Vagle and John Morrison provided help with the deployment and recovery of the moorings. Mike Dempsey and Jonathan Poole helped design and assemble the AZFP moorings. Tyler Zubkowski and Benjamin Snow participated in the DIDSON surveys. Jackie Detering and Benjamin Snow helped with the analysis of the DIDSON and the AZFP data. The Hakai foundation provided CTD data from Hoskyn channel. This project was funded through the Aquaculture Collaborative Research and Development Program (ACRDP) in association with the BC Salmon Farmers Association (BCSFA).

6 References

Barange, M. 1994. Acoustic identification, classification and structure of biological patchiness on the edge of the Agulhas Bank and its relation to frontal features. S. Afr. J. Marine Sci. 14:333-347.

Benoit-Bird, K. J. and Lawson, G.L. 2016. Ecological insights from pelagic habitats acquired using active acoustic techniques. Annu. Rev. Mar. Sci. 8:463–490.

Coetzee, J. 2000. Use of a shoal analysis and patch estimation system (SHAPES) to characterise sardine schools. Aquat. Living Resour. 13(1):1-10.

De Robertis, A., and Higginbottom, I. 2007. A post-processing technique for estimation of signal-to-noise ratio and removal of echosounder background noise. ICES J. Mar. Sci. 64:1282-1291.

De Robertis, A., McKelvey, D.R. and Ressler, P.H. 2010. Development and application of an empirical multifrequency method for backscatter classification. Can. J. Fish. Aquat. Sci. 67:1459-1474.

Dickie, L.M., Dowd, R.G. and Boudreau, P.R. 1983. An echo counting and logging system (ECOLOG) for demersal fish size distributions and densities. Can. J. Fish. Aquat. Sci. 40:487-498.

Dickie, L.M. and Boudreau, P.R. 1987. Comparison of acoustic reflections from spherical objects and fish using a dual-beam echosounder. Can. J. Fish. Aquat. Sci. 44:1915-1921.

Favali, P., Beranzoli, L. and De Santis, A. 2015. Seafloor observatories: A new vision of the earth from the abyss. Springer, Chichester, U.K. 676 pp.

Foote, K.G., Knudsen, H.P. and Vestnes, G. 1987. Calibration of acoustic instruments for fish density estimation: a practical guide. ICES Coop. Res. Rep. 144, ICES, Copenhagen 69 pp.

Foreman, M.G.G., Succhi, D.J., Garver, K.A., Tuele, D., Isaac, J., Grime, T., Guo, M. and Morrison, J. 2012. A circulation model for the Discovery Islands, British Columbia. Atmos. Ocean 50(3):301-316.

Johannesson, K.A. and Mitson, R.B. 1983. Fisheries acoustics: A practical manual for aquatic biomass estimation. FAO Fish. Tech. Paper 240, FAO, Rome, 249 pp.

Kaartvedt, S., Rostad, A., Klevjer, T.A. and Staby, A. 2009. Use of bottom-mounted echo sounders in exploring behavior of mesopelagic fishes. Mar. Ecol. Prog. Ser. 395:109-118.

Kintama. (2018). Retrieved March 29, 2018 from Kintama.com/vizualisations/

Lavery, A.C., Wiebe, P.H., Stanton, T.K., Lawson, G.L., Benfield, M.C. and Copley, N. 2007. Determining dominant scatterers of sound in mixed zooplankton populations. J. Acoust. Soc. Am. 122(6):3304-3326.

MacLennan, D.N., Magurran, A.E., Pitcher, T.J. and Hollingworth, C.E. 1990. Behavioural determinants of fish target strength. Rapp. P.-V. Réun. Cons. Int. Explor. Mer. 189:245-253.

MacLennan, D.N., Fernandes, P.G. and Dalen, J. (2002). A consistent approach to definitions and symbols in fisheries acoustics. ICES J. Mar. Sci. 59:365-369.

Parker-Stetter, S.L., Rudstam, L.G., Sullivan, P.J. and Warner, D.M. 2009. Standard operating procedures for fisheries acoustic surveys in the Great Lakes. Great Lakes Fish. Comm. Spec. Pub. 09-01

Pawlowvicz, R. and McLure, B. 2010. Inverted echosounder for continuous high-resolution water column profiling from the NEPTUNE (Canada) ocean observatory. In: Proceedings of OCEANS 2010, MTS/IEEE Seattle.

Rose, G.A. and Leggett, W.C. 1988. Hydroacoustic signal classification of fish schools by species. Can. J. Fish. Aquat. Sci. 45:597-604.

Rousseau, S., Gauthier, S., Johnson, S., Neville, C. and Trudel M., 2017. Use of inverted echosounders to monitor the migration timing and abundance of juvenile salmon in the Discovery Islands, British Columbia. Can. Tech. Rep. Fish. Aquat. Sci. 3227: viii + 33 p.

Sato, M., Dower, J.F., Kunze, E. and Dewey, R. 2013. Second-order seasonal variability in diel vertical migration timing of euphausiids in a coastal inlet. Mar. Ecol. Prog. Ser. 480:39-56.

Sato, M., Horne, J.K., Parker-Stetter, S.L. and Keister, J.E. 2015. Acoustic classification of coexisting taxa in a coastal ecosystem. Fish. Res. 172:130-136.

Simmonds, E.J., Williamson, N.J., Gerlotto, F. and Aglen, A. 1991. Survey design and data-analysis procedures: A comprehensive review of good practice. Int. Counc. Explor. Sea CMB:54, ICES, Copenhagen.

Simmonds, J. and MacLennan, D. 2005. Fisheries acoustics: theory and practice. Second Edition. Blackwell Publishing, London.

Thomson, R.E. and Allen, S.E. 2000. Time series acoustic observations of macrozooplankton diel migration and associated pelagic fish abundance. Can. J. Fish. Aquat. Sci. 57:1919-1931.

Thorpe, S.A. 1986. Measurements with an automatically recording inverted echo sounder; ARIES and the bubbles clouds. J. Phys. Oceanogr. 16:1462-1478.

Trevorrow, M.V., Vagle, S. and Farmer, D.M. 1993. Acoustical measurements of microbubbles within ship wakes. J. Acoust. Soc. Am. 95(4):1922-1930.

Trevorrow, M.V. 2003. Measurements of near-surface bubble plumes in the open ocean with implications for high-frequency sonar performance. J. Acoust. Soc. Am. 114(5):2672-2684.

Vagle, S. and Farmer, D.M. 1992. The measurement of bubble-size distributions by acoustical backscatter. J. Atmos. Oceanic. Tech. 9:630-644.